PHYS 235 Nonlinear Plasma Theory: $Ku > 1$

Lecture by Patrick Diamond, Summary by Mingyun Cao

May 30, 2022

1. Introduction

Quasi-linear theory is the simplest theory for weak plasma turbulence and instability [1]. Although quasi-linear theory seems universal, you can't mindlessly use it before confirming its applicability to the problem you are considering. In the formulation of quasi-linear theory, linearized trajectories (i.e. unperturbed orbits) of particles are used. As shown in figure 1, this is true only when the bounce time τ_b of the particle is smaller than the pattern lifetime τ_{ac} of the electric field.

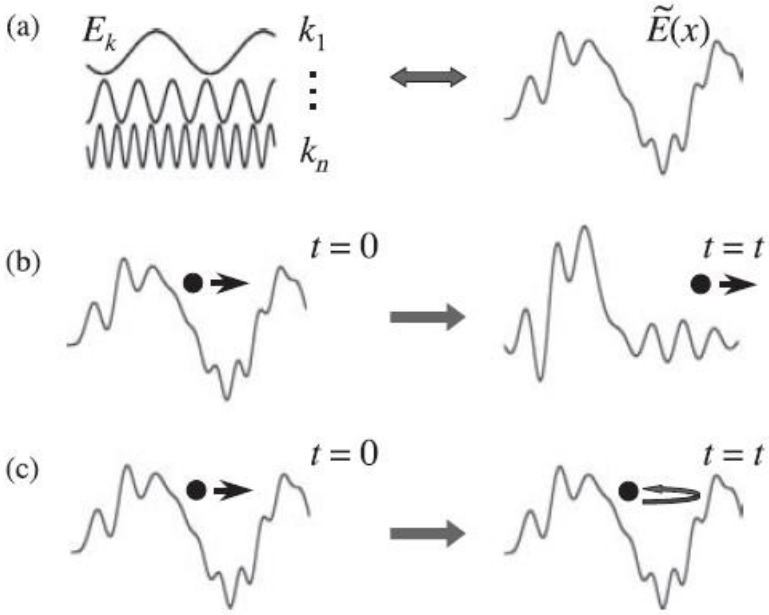

Figure 1 (a) The pattern of the electric field a particle sees at a specific time. (b) When $\tau_{ac} < \tau_b$, the pattern changes before particle bounces. In this case, it's safe to use unperturbed orbit. (c) When $\tau_{ac} > \tau_b$, particle is trapped and the direction of particle motion changes, unperturbed orbit approximation fails [1].

Therefore, the criterion for the validity of quasi-linear theory is $\tau_{ac}/\tau_b < 1$.

The idea of quasi-linear theory can also be found in the calculation of the magnetic diffusivity of stochastic magnetic fields. Recall the Liouville equation

$$\frac{\partial f}{\partial z} + \frac{B_\theta(r) + \tilde{B}_\theta}{rB_0}\frac{\partial f}{\partial \theta} + \frac{\tilde{B}_r}{B_0}\frac{\partial f}{\partial r} = 0, \qquad (1-1)$$

where f is the magnetic flux density. Equation (1-1) is the expanded form of $\boldsymbol{B}\cdot\nabla f=0$, which is the definition of flux density. It is called Liouville equation because the flow is incompressible:

$$\nabla\cdot\boldsymbol{B}=\nabla_z B_0+\nabla_\perp\cdot\boldsymbol{B}_\perp=\nabla_\perp\cdot\boldsymbol{B}_\perp=0. \tag{1-2}$$

Equation (1-1) is similar in structure to Vlasov equation. Here the coordinate in the main field direction z plays the role of time. To get the magnetic diffusivity of stochastic magnetic field, a standard quasi-linear procedure is adopted: using method of averaging to separate two different scales, finding the linear coherent response of $\tilde{f}$ to $\tilde{B}_r$, and plugging the response into the correlation $\langle\tilde{f}\tilde{B}_r\rangle$ to get D_M. The expression for D_M is [2]

$$\begin{aligned} D_M &= \left\langle -i\sum_{\boldsymbol{k},\boldsymbol{k}'}\tilde{b}_{r,\boldsymbol{k}}\tilde{b}_{r,\boldsymbol{k}'}\frac{1}{k_z-\frac{B_\theta(r)}{B_0}k_\theta}\exp[i(k_\theta+k'_\theta)\theta-(k_z+k'_z)z]\right\rangle \\ &= \pi\sum_{\boldsymbol{k}}\left|\tilde{b}_{r,\boldsymbol{k}}\right|^2\delta(k_\parallel)\approx\langle\tilde{b}_r\rangle^2 l_{ac} \end{aligned} \tag{1-3}$$

Since quasi-linear theory is used in this calculation, the validity of the result we obtain is of course restricted by the applicability of quasi-linear theory. Because we are talking about diffusion of field lines other than particles, the bouncing time of particle τ_b is replaced by the magnetic decorrelation time τ_c, or magnetic decorrelation length l_c, which is the distance that two originally adjacent field lines traveled before they diverged. More specifically, we require

$$Ku=\frac{\delta_r}{\Delta_r}=\frac{\tilde{B}_r}{B_0}\frac{l_{ac}}{\Delta_r}\approx\left(\frac{l_{ac}}{l_c}\right)^2<1, \tag{1-4}$$

where Ku is called Kubo number, δ_r is the radial auto-correlation length, Δ_r is the radial decorrelation length, l_{ac} is the parallel auto-correlation length which is inversely proportional to the bandwidth of $k_\parallel$. Obviously, equation (1-4) and the criterion $\tau_{ac}/\tau_b<1$ are essentially the same.

This magnetic diffusivity D_M is widely used in theories relevant to stochastic magnetic field [2,3], which means the validity of all these theories can only be justified when $Ku<1$. Studies on stochastic magnetic field have practical significance for magnetic confinement fusion. Nowadays resonant magnetic perturbation (RMP) is widely applied to generate a stochastic magnetic field to mitigate and suppress edge localized mode (ELM). However, RMP also raises the power threshold

of L-H transition. Therefore, good confinement is no longer deemed sufficient. *On the contrary, we need to reconcile good confinement with good power handling.* That's why understanding plasma dynamics in a stochastic magnetic field is of great importance to magnetic confinement fusion. Unfortunately, most of the studies so far only focus on $Ku < 1$ regime, whereas the real case in tokamak is $Ku{\sim}1$. Therefore, it would be beneficial to probe into the world of $Ku{\sim}1$ from another direction, i.e., extending theories on $Ku > 1$ regime to $Ku{\sim}1$ regime. As shown in figure 2, what we are interested in is the tiny space between Adam and God's fingertips, which is the origin of all the miracles. Clearly, only Adam and God, the only two witnesses to this exciting moment, know what happened there. But for a long time, humanity only observe that mysterious area from Adam's side. *Now, it's time to step into the realm of God and detect that* $Ku{\sim}1$ *regime from God's perspective.*

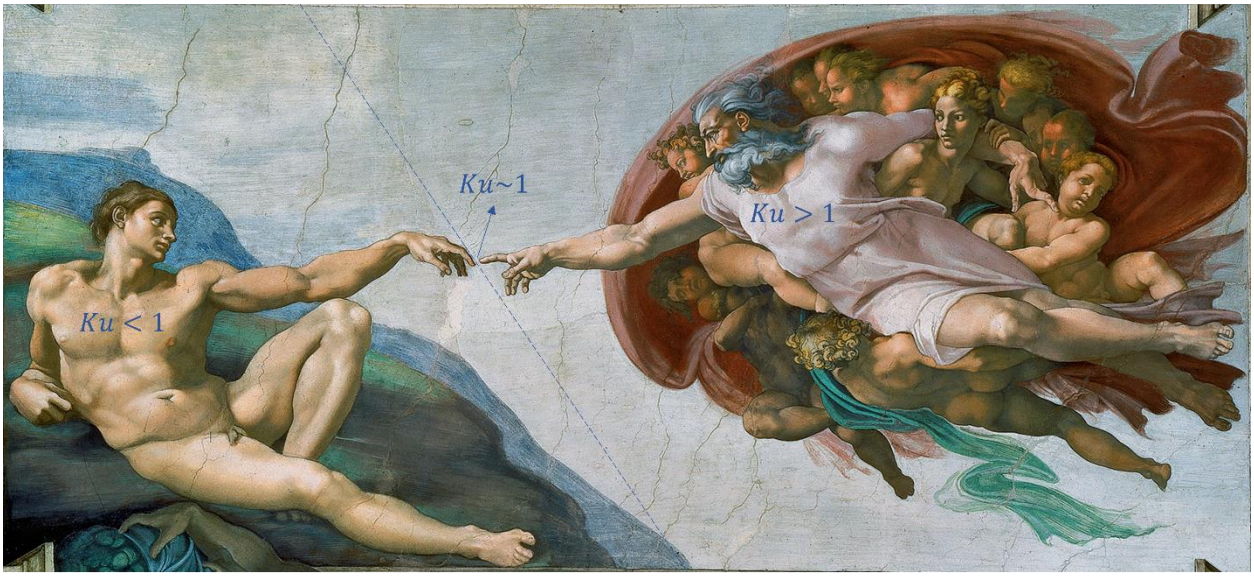

Figure 2 Perspectives from Adam and God on the origin of everything

So this note aims to give a brief introduction to theories on $Ku > 1$ physics. As discussed in section 2, $Ku > 1$ indicates that the nonlinear scattering process controls the spatial and temporal scales. We first assume that this nonlinear process doesn't change the diffusion essence of the system and calculate the effective diffusivity via resonance broadening theory (RBT). Out of my personal interest, I'd like to give a more systematic introduction of RBT in this section. However, we can show that diffusion is inappropriate to describe this kind of systems. Instead, characteristics of these systems are more like percolation process. So in section 4 we will introduce basics of percolation theory. In addition to what Pat taught in his lectures, I'd like to show how to use

renormalization group theory to calculate the scaling exponents and critical occupation probability of 2D triangular lattice. Models in section 3 are intermediate between diffusion and percolation, i.e., an array of convective cells or a shear flow plus a global diffusion.

2. Diffusion in two-dimensional disordered systems

When $Ku < 1$, the expression for magnetic diffusivity is

$$\begin{aligned} D_M &= \int_0^\infty dl \langle \tilde{b}_r(0)\tilde{b}_r(l)\rangle \\ &= \int_0^\infty dl \sum_{\boldsymbol{k}} \left|\tilde{b}_{r,\boldsymbol{k}}\right|^2 e^{ik_\parallel l} \\ &\approx \sum_{\boldsymbol{k}} \left|\tilde{b}_{r,\boldsymbol{k}}\right|^2 \frac{1}{k_\parallel} \approx \langle \tilde{b}_r \rangle^2 l_{ac} \end{aligned} \quad , \qquad (2-1)$$

which is just another form of equation (1-3). Recall the definition of Kubo #, we can rewrite it as

$$Ku \sim \frac{\tilde{B}_r}{B_0}\frac{l_{ac}}{\Delta_\perp} \sim \frac{l_{ac}}{l_{NL}}, \qquad (2-2)$$

where $l_{NL}^{-1} \sim \tilde{B}_r/B_0\partial_r$ is the nonlinear mixing length. It corresponds to the third term of equation (1-1). *Therefore, in large Kubo regime, nonlinear scattering process dominates and sets the spatial and temporal scales.* Similar stories occur in turbulent flow and collisional drift wave. For turbulent flow, we can define Kubo # as

$$Ku \sim \frac{\tau_{ac}\tilde{v}}{\Delta} \sim \frac{\tau_{ac}}{\tau_{NL}}, \qquad (2-3)$$

where τ_{NL} is the eddy circulation time. For collisional drift wave, Kubo # and the auto-correlation time are defined as

$$Ku \sim \frac{\tau_{ac}}{\tau_{NL}}, \qquad \tau_{ac} \sim \frac{1}{\Delta\left|\chi_\parallel k_\parallel^2\right|}. \qquad (2-4)$$

Two natural examples for $Ku \gg 1$ are two-dimensional guiding center plasma and a random array of discrete charged rods [4]. As shown in figure (3), both of them are translationally invariant in the main field direction, which indicates an infinite l_{ac} and an infinite Kubo number. We want to calculate the effective diffusivity of these two models under nonlinear scattering correction.

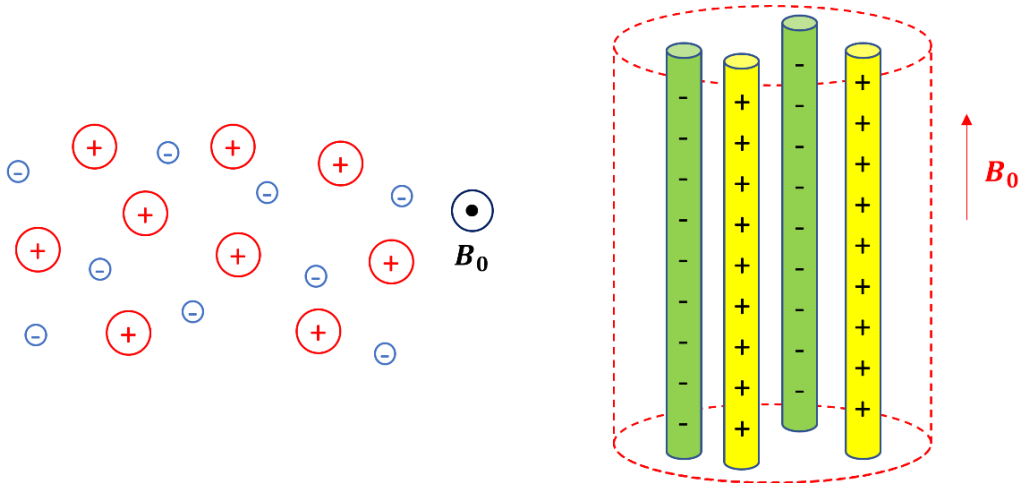

Figure 3 Illustrations of 2D guiding center plasma and a random array of charged rods. They are both translationally invariant along the main field and disordered in the plane perpendicular to main field.

The model of 2D guiding center plasma consists of two equations

$$\frac{\partial}{\partial t}\rho + \frac{\nabla\varphi \times \hat{\boldsymbol{z}}}{B_0}\cdot\nabla\rho = D_0\nabla^2\rho, \tag{2-5}$$

$$\nabla^2\varphi = -4\pi\rho. \tag{2-6}$$

Then, the effective diffusion coefficient of integral of correlation is given by

$$\langle D_\perp\rangle \cong \int_0^\infty d\tau\langle\tilde{v}(0)\tilde{v}(\tau)\rangle \sim \int_0^\infty d\tau\sum_{\boldsymbol{k}}|\tilde{v}_{\boldsymbol{k}}|^2\langle R(\tau)\rangle, \tag{2-7}$$

which is similar in form to equation (2-1). However, in equation (2-7), the memory function $R(\tau)$ not only contains the unperturbed orbit, but also contains the nonlinear scattering, i.e.,

$$R(\tau) = e^{-i\boldsymbol{k}_\perp\cdot\boldsymbol{r_0}}e^{\underbrace{i\left[(\omega-k_\parallel v_\parallel)\tau+\boldsymbol{k}_\perp\cdot\boldsymbol{r_0}\right]}_{unperturbed\ orbit}+\underbrace{i\boldsymbol{k}_\perp\cdot\boldsymbol{\delta r}(-\tau)}_{NL\ scattering}}. \tag{2-8}$$

From equation (2-8) we can see, the linear wave-particle resonance is broadened by the nonlinear effect. This is a typical example of *resonance broadening theory*. Because $Ku \to \infty$, $\omega, k_\parallel \to 0$. And since the nonlinear scattering is stochastic, only average diffusion coefficient is of physical significance. That's why we take the ensemble average (denoted by bracket $\langle\rangle$) in equation (2-7). One of basic assumptions of resonance broadening theory is that particle orbits are stochastic, so we can expand $R(\tau)$, take its ensemble average, and then obtain (*here the pdf of* $\boldsymbol{\delta r}$ *is a Gaussian*)

$$\begin{aligned}\langle R(\tau)\rangle &= \left\langle e^{i\boldsymbol{k}_\perp\cdot\boldsymbol{\delta r}(-\tau)}\right\rangle \\ &= \left\langle 1+\underbrace{i\boldsymbol{k}_\perp\cdot\boldsymbol{\delta r}(-\tau)}_{=0}-\frac{1}{2}\left(\boldsymbol{k}_\perp\cdot\boldsymbol{\delta r}(-\tau)\right)^2+\cdots\right\rangle. \\ &\cong \left\langle 1-\frac{(\boldsymbol{k}_\perp\cdot\boldsymbol{\delta r})^2}{2}\right\rangle \cong 1-k_\perp^2\langle D_\perp\rangle\tau\cong e^{-k_\perp^2\langle D_\perp\rangle\tau}\end{aligned} \qquad (2-9)$$

Plugging equation (2-9) into equation (2-7), we get

$$\langle D_\perp\rangle=\int_0^\infty d\tau\sum_{\boldsymbol{k}}|\tilde{v}_{\boldsymbol{k}}|^2e^{-k_\perp^2\langle D_\perp\rangle\tau}=\sum_{\boldsymbol{k}}|\tilde{v}_{\boldsymbol{k}}|^2\frac{1}{k_\perp^2\langle D_\perp\rangle}. \qquad (2-10)$$

Here comes some observations.

- The characteristic time of nonlinear scattering τ_c is $1/k_\perp^2\langle D_\perp\rangle$. τ_c is controlled by $\langle D_\perp\rangle$ and it becomes large at large spatial scale. *This is because of the "slow mode" originating from the conservation of ρ, i.e. $\partial_t\int\rho d^2x\to 0$.* Here ρ is called "conserved order parameter".
- $\langle D_\perp\rangle$ is defined recursively, which is a symbol of a strong scattering process.
- Because $\tilde{v}$ here is $E\times B$ drift velocity fluctuation, $\langle D_\perp\rangle\propto 1/B_0$, the scaling law of Bohm diffusion.

Assuming a symmetric spectrum, we get

$$\langle D_\perp\rangle=\left(\sum_{\boldsymbol{k}}\frac{|\tilde{v}_{\boldsymbol{k}}|^2}{k_\perp^2}\right)^{\frac{1}{2}}\approx\frac{c}{B_0}\left(\int dk_\perp\frac{|E_{\boldsymbol{k}}|^2}{k_\perp}\right)^{\frac{1}{2}}. \qquad (2-11)$$

To proceed, we need to know the spectrum of the fluctuating electric field.

By using *test particle model* (TPM)[1], we can obtain the spectrum of 2D guiding center plasma,

[1] What is test particle model? A test particle model is a plasma kinetics theory to calculate the fluctuation spectrum and relaxation rate in a near-equilibrium plasma, which is characterized by a balance of emission and absorption by particles at a rate related to the temperature T , the validity of linear response theory, and the use of linearized particle trajectories. In many cases, plasma is viewed as Vlasov fluid. However, since plasma is composed by isolated particles (like a pea soup), the probability distribution function has many spikes displaying the discreteness of particles. As evidence of this argument, these spikes disappear if we divide each particle into many smaller particles (i.e., crushing peas in a pea soup) while keeping charge conservation. These spikes can be treated as quasi-particles and emit radiation as moving through plasma. This radiation will be absorbed by plasma via Landau damping. Thus, in TPM, each particle can stimulate a collective response from the other particle by its discreteness and respond to or "dresses" other discrete particles by forming part of the background Vlasov fluid. In other words, each particle has a dual identity, both as an emitter and an absorber.

which is

$$|E_{\boldsymbol{k}}|^2 = \frac{4\pi}{l}\frac{k_B T}{1+k_\perp^2\lambda_D^2} = \frac{4\pi}{e}\frac{e}{l}\frac{k_B T}{1+k_\perp^2\lambda_D^2}, \tag{2-13}$$

where l is the parallel scale length, λ_D is the Debye length. Plugging equation (2-13) into equation (2-11), we obtain

$$\begin{aligned} D_\perp &\sim \frac{c}{B_0}\left(\int_{1/L_0}^{1/\lambda_D} dk_\perp \frac{4\pi}{e}\frac{e}{l}\frac{k_B T}{(1+k_\perp^2\lambda_D^2)k_\perp}\right)^{1/2} \\ &\sim \frac{ck_B T}{eB_0}\left[\frac{\ln(L/\lambda_D)}{n\lambda_D^2}\right]^{1/2} = D_B\left[\frac{\ln(L_0/\lambda_D)}{n\lambda_D^2}\right]^{1/2}. \end{aligned} \tag{2-14}$$

The upper bound of the integral is $1/\lambda_D$ since λ_D is the smallest scale. And since the perpendicular system size L_0 is the largest scale, the lower bound of the integral is $1/L_0$.

As for a random array of charged rods, we have Poisson's equation

$$\nabla \cdot \boldsymbol{E} = 4\pi \sum_i \frac{q_i}{l}\delta(\boldsymbol{x}-\boldsymbol{x_i}). \tag{2-15}$$

Taking the Fourier transform of equation (2-15), we get

$$i\boldsymbol{k}\cdot\boldsymbol{E_k} = \frac{4\pi}{l}\sum_i q_i e^{-\boldsymbol{k}\cdot\boldsymbol{x_i}}. \tag{2-16}$$

Then we have

$$|E_{\boldsymbol{k}}|^2 = \frac{1}{k_\perp^2}\left(\frac{4\pi}{l}\right)^2\left\langle\sum_{i,j} q_i q_j e^{i\boldsymbol{k}\cdot(\boldsymbol{x_j}-\boldsymbol{x_i})}\right\rangle = \frac{16\pi^2 nq^2}{k_\perp^2 l^2}. \tag{2-17}$$

Plugging equation (2-17) into equation (2-11), we obtain

$$D_\perp \sim \frac{c}{B_0}\left[\int_{1/L_0}^{1/\lambda_D} dk_\perp \frac{16\pi^2 nq^2}{k_\perp^3 l^2}\right]^{1/2} \sim \frac{ck_B T}{B_0}\left[\frac{L_0^2}{n\lambda_D^4}\right]^{1/2} = D_B\left[\frac{L_0^2}{n\lambda_D^4}\right]^{1/2}. \tag{2-18}$$

Both of equation (2-14) and equation (2-18) recover the scaling of Bohm diffusion and have a dependence on the macroscopic scale L_0, which arises from the "slow mode", i.e., $\tau_c \to \infty$ as

$k_\perp \to 0$. *Clearly the macro-scale dependence of the random array is stronger.*

Can we generalize the results of equation (2-14) and equation (2-18) to stochastic magnetic field with $Ku > 1$? We have already seen the similarity between equation (2-1) and equation (2-7). To make this point clearer, we can write down the equations of motion of 2D guiding center plasma

$$\begin{aligned} \frac{dx}{dt} &= -\frac{c}{B}\frac{\partial \varphi}{\partial y}, \\ \frac{dy}{dt} &= \frac{c}{B}\frac{\partial \varphi}{\partial x}. \end{aligned} \tag{2-19}$$

In the $Ku \to \infty$ limit, $l_{ac} \to \infty$, so stochastic magnetic field is homogeneous in z direction and random in x and y directions, just like the random array of charged rods. The trajectory of a field line satisfies

$$\frac{dx}{\tilde{B}_x} = \frac{dy}{\tilde{B}_y} = \frac{dz}{B_0}. \tag{2-20}$$

So

$$\begin{aligned} \frac{dx}{dz} &= \tilde{b}_r = \frac{\partial A}{\partial y}, \\ \frac{dy}{dz} &= \tilde{b}_\theta = -\frac{\partial A}{\partial x}. \end{aligned} \tag{2-21}$$

Obviously, equation (2-19) and equation (2-21) are same in structure, whereas in equation (2-21) z plays the role of t. Therefore, it is safe to extend the calculation of D_M to include resonance broadening. Following equation (2-1) and equation (2-7), the magnetic diffusivity is

$$\begin{aligned} \langle D_M \rangle &= \int_0^\infty dl \langle \tilde{b}(0)\tilde{b}(l) \rangle = \sum_{\boldsymbol{k}} \int_0^\infty dl \left|\tilde{b}_{\boldsymbol{k}}\right|^2 e^{ik_\parallel l} \left\langle e^{i\boldsymbol{k}\cdot\boldsymbol{\delta r}(-l)} \right\rangle \\ &= \sum_{\boldsymbol{k}} \int_0^\infty dl \left|\tilde{b}_{\boldsymbol{k}}\right|^2 e^{ik_\parallel l} e^{-k_\perp^2 \langle D_M \rangle l} = \sum_{\boldsymbol{k}} \left|\tilde{b}_{\boldsymbol{k}}\right|^2 \frac{i}{k_\parallel + \underbrace{ik_\perp^2 \langle D_M \rangle}_{\substack{resonance \\ broadening}}}, \end{aligned} \tag{2-22}$$

where the unperturbed trajectory is kept. Taking the real part of equation (2-22), we get

$$Re\langle D_M \rangle = \sum_{\boldsymbol{k}} \left|\tilde{b}_{\boldsymbol{k}}\right|^2 \frac{k_\perp^2 \langle D_M \rangle}{k_\parallel^2 + (k_\perp^2 \langle D_M \rangle)^2}, \tag{2-23}$$

where $k_\perp^2 D_M/k_\parallel \sim Ku^2$.

For $Ku \ll 1$, we restore the result of equation (1-3). For $Ku \gg 1$, equation (2-33) reduces to

$$\langle D_M \rangle = \sum_{\boldsymbol{k}} \frac{\left|\tilde{b}_{\boldsymbol{k}}\right|^2}{k_\perp^2 \langle D_M \rangle}. \qquad (2-24)$$

Since $|A_{\boldsymbol{k}}|^2 = \left|\tilde{b}_{\boldsymbol{k}}\right|^2 k_\perp^2$, we obtain

$$\langle D_M \rangle \sim \left\langle \tilde{b}^2 \right\rangle^{1/2} \Delta. \qquad (2-25)$$

Above discussions and calculations involve the idea of resonance broadening theory [1]. Here I'd like to use wave-particle interaction as an example to give a more detailed introduction to resonance broadening theory. First, regarding its name, there are two questions we need answer. Resonance between what and what? And the resonance is broadened by what? *For wave-particle interaction, of course, it is the resonance between a wave and its corresponding resonant particles. This resonance can be broadened by other background modes. For the diffusion of field lines, magnetic perturbation is resonant with the magnetic surface which has the same pinch rate. And this resonance is broadened by other magnetic perturbations*. Then what does "broadening" mean? We will answer this question later.

As quasi-linear theory answering the question "How does $\langle f \rangle$ evolve in the presence of a spectrum of waves, given that the particle orbits are stochastic?", resonance broadening theory answers the question "How does the plasma distribution function f respond to a test wave $E_{k,\omega}$ at (k, ω), given an existing spectrum of background wave?" In other words, resonance broadening theory aims to find the modification of background wave to the linear response of $f_{k,\omega}$ to $E_{k,\omega}$.

Resonance broadening theory replies upon two assumptions:

- Particle orbits are assumed to be stochastic, so excursions from unperturbed orbits may be treated as diffusion process. We have already used this assumption to calculate the ensemble average of the memory function in equation (2-9).
- The "test wave" approximation is assumed to be valid. This approximation is similar to test particle model. As shown in figure 4, it means that the ensemble of interacting modes is sufficiently large and statistically homogeneous so that removing any test mode does not alter

the physics of the ensemble of remaining modes.

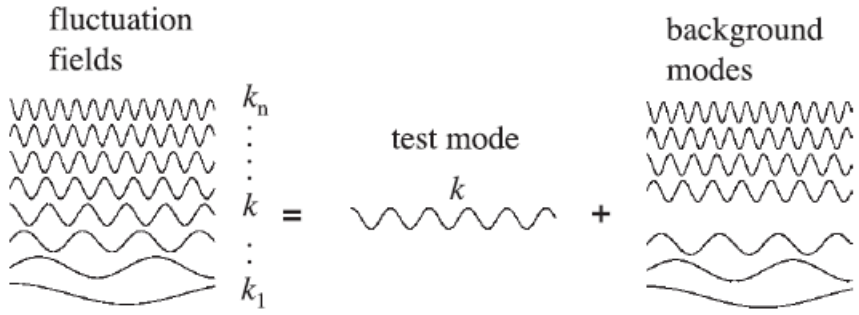

Figure 4 Test wave approximation, we can remove on test mode without changing the physics of the ensemble of other background modes [1].

The idea of resonance broadening theory is like that of Weiner-Feynman path integral, i.e., replacing the integration over the time history of the exact (or "perturbed") orbit by an average over a statistical ensemble of excursions from the linear (or "unperturbed") orbit, as depicted in figure 5.

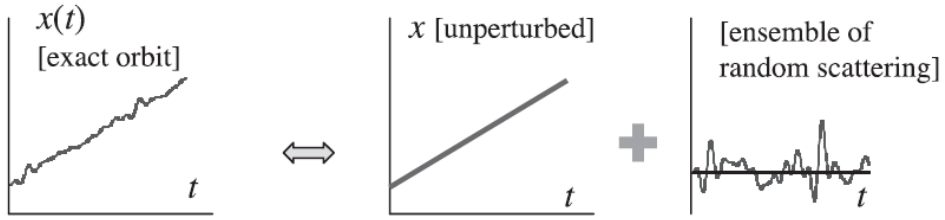

Figure 5 In resonance broadening theory, an exact orbit can be regarded as a superposition of an unperturbed orbit and an ensemble of random scattering [1].

Rewriting the linearized Vlasov equation as

$$\frac{df_k}{dt} = -\frac{q}{m}E_k\frac{\partial\langle f\rangle}{\partial v}, \qquad (2-26)$$

where d/dt is determined by the characteristic equations (of the Vlasov equation),

$$dx/dt = v, \qquad dv/dt = qE/m. \qquad (2-27)$$

At $t = 0$, $f_k e^{ikx} = f_{k,\omega}e^{ikx}e^{i\omega t}|_{t=0} = f_{k,\omega}e^{ikx}$. Since $E_k = E_{k,\omega}e^{i\omega t}$, multiplying equation (2-16) by e^{ikx} and integrating it over time (tracing back the orbit), we obtain

$$f_{k,\omega} = -\frac{q}{m}e^{-ikx}\int_0^\infty d\tau e^{i\omega\tau}U(-\tau)\left[e^{ikx}E_{k,\omega}\frac{\partial\langle f\rangle}{\partial v}\right], \qquad (2-28)$$

where $U(-\tau)$ is the formal, exact orbit propagator, which has the property that

$$U(-\tau)x = x(-\tau) = x_0(-\tau) + \delta x(-\tau) = x_0 - v\tau + \delta x(-\tau). \qquad (2-29)$$

Plugging equation (2-29) into equation (2-28), we get

$$f_{k,\omega} = -\int_0^\infty d\tau e^{i(\omega - kv)\tau} e^{ik\delta x(-\tau)} \frac{q}{m} E_{k,\omega} \frac{\partial \langle f \rangle}{\partial v}. \qquad (2-30)$$

In resonance broadening theory, $f_{k,\omega}$ is replaced by its ensemble average, i.e.,

$$f_{k,\omega} \to \langle f_{k,\omega} \rangle_{OE} = -\int_0^\infty d\tau e^{i(\omega - kv)\tau} \langle e^{ik\delta x(-\tau)} \rangle \frac{q}{m} E_{k,\omega} \frac{\partial \langle f \rangle}{\partial v}. \qquad (2-31)$$

To calculate $\langle e^{ik\delta x(-\tau)} \rangle$, we note that

$$\delta x(-\tau) = -\int_0^\tau d\tau' \delta v(-\tau'), \qquad (2-32)$$

and

$$\langle e^{ik\delta x(-\tau)} \rangle_{OE} = \left\langle \exp\left[-ik \int_0^\tau \delta v(-\tau') d\tau' \right] \right\rangle_{OE}. \qquad (2-33)$$

Excursions in velocity are produced by fluctuating electric fields of the turbulent wave ensemble, i.e., $d\delta v/dt = q\tilde{E}/m$. Since the ensemble of waves is homogeneous, it is reasonable to assume a Gaussian pdf of $\tilde{E}$, so that δv behaves diffusively, i.e.,

$$pdf[\delta v] = \frac{1}{\sqrt{\pi D \tau}} \exp[-\delta v^2 / D\tau]. \qquad (2-34)$$

Thus we can define the ensemble average as

$$\langle A \rangle_{OE} = \int \frac{d\delta v}{\sqrt{\pi D \tau}} \exp[-\delta v^2 / D\tau] A. \qquad (2-35)$$

Using this definition, equation (33) reduces to

$$\langle e^{ik\delta x(-\tau)} \rangle_{OE} = \exp\left[-\frac{k^2 D \tau^3}{6} \right]. \qquad (2-36)$$

Plugging equation (2-36) into equation (2-31), we get

$$\langle f_{k,\omega}\rangle = -\int_0^\infty d\tau \exp\left[i(\omega - kv)\tau - \frac{k^2 D\tau^3}{6}\right]\frac{q}{m}E_{k,\omega}\frac{\partial\langle f\rangle}{\partial v}. \qquad (2-37)$$

We can define $\tau_c = (k^2 D/6)^{-1/3}$, so equation (2-37) becomes

$$\langle f_{k,\omega}\rangle = -\int_0^\infty d\tau \exp\left[i(\omega - kv)\tau - \frac{\tau^3}{\tau_c^3}\right]\frac{q}{m}E_{k,\omega}\frac{\partial\langle f\rangle}{\partial v}. \qquad (2-38)$$

This result is slightly different from equation (2-9) and equation (2-22), because it is velocity, not position, that is scattered by electric field fluctuations. To some extent, this result is more accurate compared with equation (2-9) and equation (2-22), though for simplicity we still assume δr behaves diffusively in many calculations. If we adopt this approximation, τ^3/τ_c^3 is replaced by τ/τ_c, and equation (2-38) is modified to

$$\langle f_{k,\omega}\rangle = -\frac{i}{\left(\omega - kv + \frac{i}{\tau_c}\right)}\frac{q}{m}E_{k,\omega}\frac{\partial\langle f\rangle}{\partial v}. \qquad (2-39)$$

Taking the real part of equation (2-39), we get

$$Re\langle f_{k,\omega}\rangle = -\frac{1/\tau_c}{(\omega - kv)^2 + 1/\tau_c^2}\frac{q}{m}E_{k,\omega}\frac{\partial\langle f\rangle}{\partial v}. \qquad (2-40)$$

In the limit of $1/\tau_c \to 0$, i.e., completely ignoring the correction of nonlinear broadening, we recover the result of quasi-linear theory

$$Re\langle f_{k,\omega}\rangle = -\pi\delta(\omega - kv)\frac{q}{m}E_{k,\omega}\frac{\partial\langle f\rangle}{\partial v}. \qquad (2-41)$$

Now, the meaning of "broadening" becomes clear. The effect of scattering by the turbulent spectrum of background waves is to broaden the linear wave-particle resonance, from a delta function of zero width in quasi-linear theory to a function of finite width proportional to $1/\tau_c$.

All the results calculated in this section can be regarded as applications of resonance broadening theory. However, we can question the correctness of these results by doubting basic assumptions of resonance broadening theory, i.e., *is it reasonable to assume that excursions from unperturbed orbits can be treated as a diffusion process?*

Recall equation (2-21), it can be simplified to

$$\nabla A \cdot d\boldsymbol{x} = 0. \qquad (2-42)$$

In other words, magnetic field lines are contours of constant A, as in a topographical map (see figure 6).

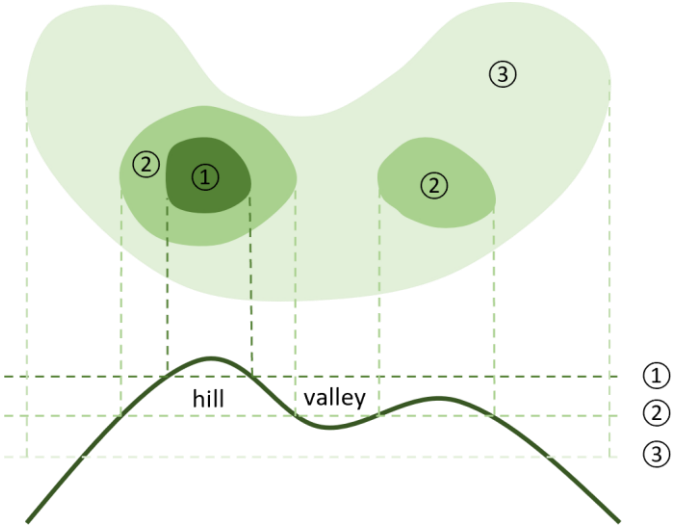

Figure 6 Contours of A. As we can expect, most of the contours are localized and closed, as (1) and (2). They contribute little to transport. However, contours like (3) span the system and contribute a lot to the transport.

We can set $\langle A \rangle = 0$, $\langle A^2 \rangle = A_0^2$, where $\langle\rangle$ denotes ensemble average [5]. Therefore, A_0 is the average height or depth of a hill or a valley. As illustrated in figure 6, most contours, like (1) and (2), are closed and isolated, thus give little contribution to transport. But contours along "passes", like (3), can take long path lengths. Transport occurs primarily along there. As shown in figure 7, for a system with a temperature gradient (like a tokamak), transport can only happen along contours like (c). So if this picture is true, we may find sharply localized strike marks at plasma-facing component of a tokamak. This is essentially different from diffusion process, which may lead to a uniform distribution of erosion. As $A \to 0$, length of island or isoline surrounding island scales as

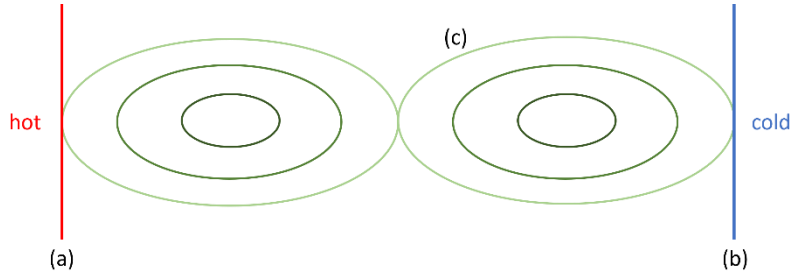

Figure 7 Heat transport can only happen at channels like contour (c)

$$l_A \sim A^{-\gamma}. \qquad (2-43)$$

Therefore, it is more like a percolation process rather than a diffusion process! Since one of the pillars of resonance broadening theory now collapses in this case, we need to study percolation theory to understand the physics of $Ku > 1$ regime.

The table below shows the difference between percolation and diffusion.

	Medium	Particle Motion
Percolation	Random	Deterministic
Diffusion	Fixed	Stochastic

Table 1 Differences between Percolation and Diffusion

For example, in 1D random walk, the medium is uniform. Each step has the same probability of going left and right. The mean squared displacement $\langle x^2 \rangle$ is proportional to step number N. In contrast, in 1D percolation, each site is assigned a left or right orientation with probability $1/2$. So the medium itself is stochastic. Given the initial condition of a particle, its trajectory is uniquely determined, as shown in figure 8.

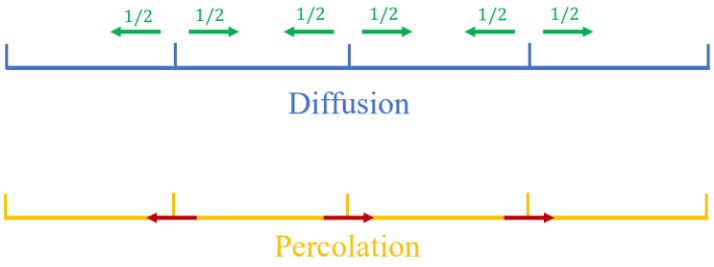

Figure 8 1D random walk vs. 1D percolation

3. Side stories: Taylor cell problem and Taylor shear dispersion

Before we formally introduce percolation theory, it is useful to study models intermediate between diffusion and percolation. Closed field lines in figure 7 can be seen as convective cells. In such a system, the motion of particles is deterministic, i.e., they always move along field lines. However, if two cells are close enough, collisional diffusion can kick particles from one cell to another. Therefore, a small but finite global diffusion makes a nontrivial difference.

A typical example is Taylor cell problem [6]. As depicted in figure 9, consider an array of convective cells. These cells marginally overlap each other. The system has a global density gradient from right to left. Therefore, particles tend to move from left to right to release stored free

energy. However, the rotate speed of these vortices is so fast that they can capture and trap particles easily. But if we introduce a global diffusion D_0, particles can be kicked off a streamline at the narrow gap between two convective cells. *This diffusion is the ultimate origin of irreversibility*. Clearly, there are two different time scales: fast convection operating in cells and slow diffusion operating in boundary layers. We can define a dimensionless number to quantify the degree of time scale separation. For a passive scalar, it satisfies

$$\frac{\partial n}{\partial t} + \boldsymbol{v} \cdot \nabla n - D_0 \nabla^2 n = 0. \qquad (3-1)$$

The ratio of the second term to the third term defines a Peclet number

$$Pe = \frac{v_0 l_0}{D_0}. \qquad (3-2)$$

In this case, since the convection is much faster than diffusion, $Pe \gg 1$.

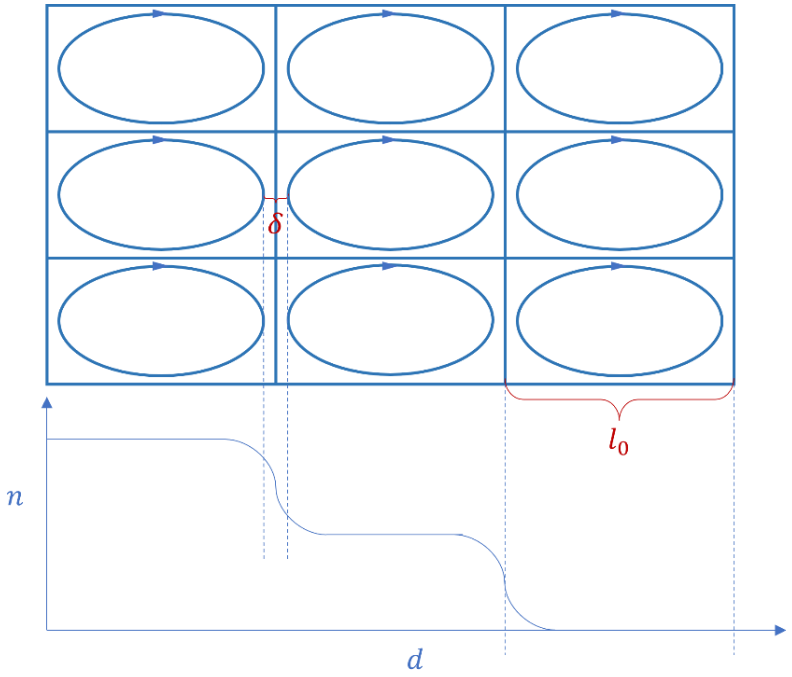

Figure 9 The configuration and density profile of Taylor cell problem

Because the diffusion process is slow, it is not a surprise to see the density profile looks like a staircase. Here we assume the characteristic scale of cells is l_0, the width of boundary layer is δ and $\delta \ll l_0$. We are interested in the effective diffusivity for scales much larger than l_0. In MFE, when we calculate effective diffusivity, we simply take the summation of turbulent diffusivity and neoclassical diffusivity. But as we will see, the effective diffusivity of Taylor cell problem is the

geometric mean of D_0 and $D_{convction}$.

For a random walk, diffusion coefficient is calculated by $(\Delta x)^2/\Delta t$. In this case, the time step is l_0/v_0, the cell circulation time, and the step size is l_0. *Nevertheless, since diffusion only happens in boundary layer, to calculate D_{eff}, we need to multiply $(\Delta x)^2/\Delta t$ by a factor $f_{active} = \delta/l_0$, which is the ratio of the active volume to the total volume.* So heuristically,

$$D_{eff} \cong f_{active}\frac{(\Delta x)^2}{\Delta t} = \frac{\delta}{l_0}\frac{l_0^2}{\frac{l_0}{v_0}} = \delta v_0. \qquad (3-3)$$

To further simplify equation (3-3), we need to calculate δ. Since particles undergo a pure random walk in boundary layer, we can calculate δ by

$$\delta^2 = D_0\Delta t = D_0\frac{l_0}{v_0}. \qquad (3-4)$$

Plugging equation (3-4) into equation (3-3), we obtain

$$D_{eff} = \sqrt{D_0 v_0 l_0} = \sqrt{D_0 D_{convection}} = \sqrt{D_0^2 Pe} = D_0(Pe)^{1/2}. \qquad (3-5)$$

Again, it is worth emphasizing that this result is not a simple addition, but a geometric mean.

Another related and interesting model is Taylor shear dispersion. This phenomenon was first discovered by G.I. Taylor in 1953 [7]. As shown in figure 10, this problem is stated by a comparison of three laminar flows, into which dye with molecular diffusion D_0 is integrated.

In figure 10(a), when there is no flow, we expect that the evolution of the radius of the dye follows

$$\delta r \sim \sqrt{D_0 t}. \qquad (3-6)$$

In figure 10(b), the flow is static and uniform since we adopt a slip boundary condition. Because the perpendicular motion of dye molecules is restricted, after $t \gg L_\perp^2/D_0$, the diffusion of the dye will saturate in the y direction. The shape of the dye transits from a circle to a slug, which expands axially at the rate of $(D_0 t)^{1/2}$ and advects at the speed of v_0.

So far, nothing is fancy. But what if we change the boundary condition to a no-slip boundary condition? In this situation, the profile of the flow becomes a parabola, i.e., $\bar{v}_x(y) = 2v_0(1 -$

$y^2/L_\perp^2$). As illustrated in figure 10(c), Taylor found in his experiments that there is a more rapid dispersal of dye in shear flow, i.e., effective axial diffusion enhanced ($D_{eff,axial} > D_0$) after $t \gg L_\perp^2/D_0$. Now the question is: *what is effective along stream diffusivity of passive scalar in a laminar*

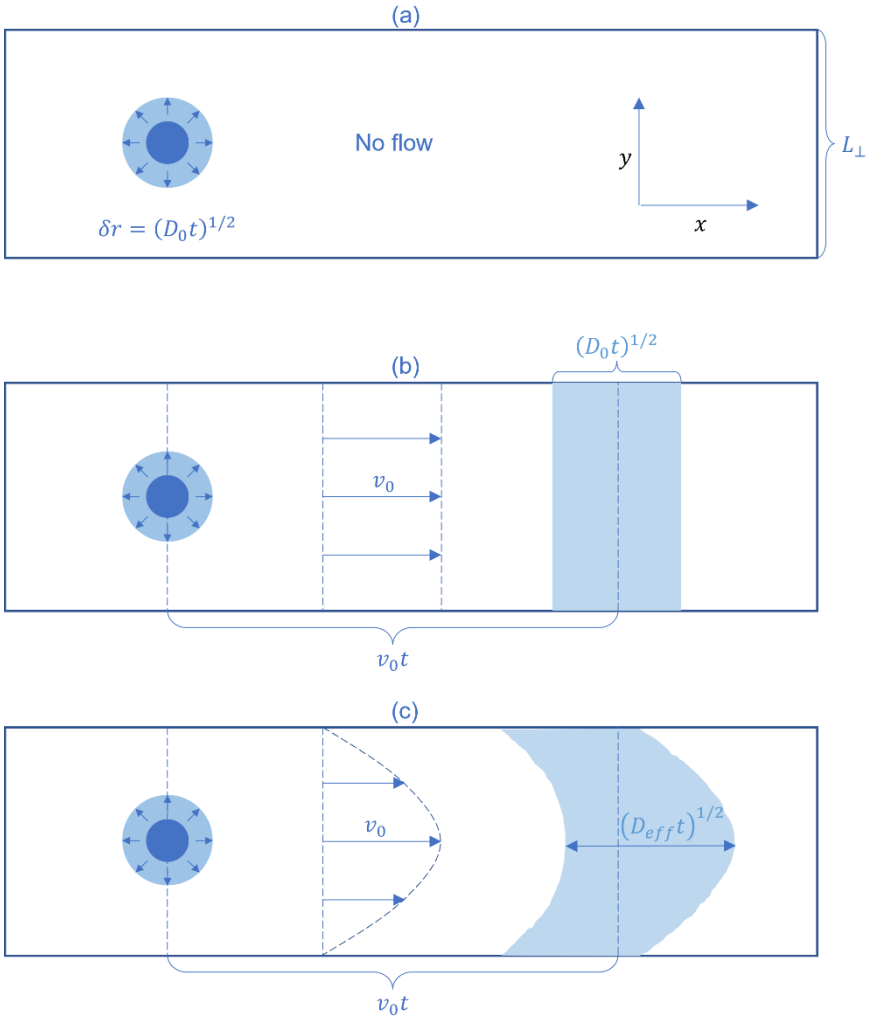

Figure 10 Taylor shear dispersion. (a) In the case of no flow, the dye undergoes a diffusion process. (b) In the case of uniform flow, the dye becomes a slug which advects at the speed of v_0 and expands at the rate of $(D_0 t)^{1/2}$ after $t \gg L_\perp^2/D_0$. (c) In the case of shear flow, a more rapid dispersal of the dye happens in the axial direction.

shear flow?

Recall equation (3-1). Because we are interested in axial diffusion and due to the time scale separation, we can take the average of n and $\boldsymbol{v}$ over the lateral direction and get

$$\begin{aligned}\langle n\rangle &= \frac{1}{L_\perp}\int_{-L_\perp/2}^{L_\perp/2} n(x,y,t)dy \\ \langle \boldsymbol{v}\rangle &= \frac{1}{L_\perp}\int_{-L_\perp/2}^{-L_\perp/2} \boldsymbol{v}(x,y)dy\end{aligned}, \qquad (3-7)$$

where n and $\boldsymbol{v}$ are concentration of dye molecules and velocity field respectively. Then n and $\boldsymbol{v}$ can be decomposed into a mean part and a fluctuation part, i.e.,

$$\begin{aligned} n &= \langle n\rangle + \tilde{n}, \\ \boldsymbol{v} &= \langle \boldsymbol{v}\rangle + \tilde{\boldsymbol{v}}. \end{aligned} \qquad (3-8)$$

Substituting equation (3-8) into equation (3-1), and taking the spatial average over y, we obtain

$$\begin{aligned} &\frac{\partial}{\partial t}\langle n\rangle + \langle v_x\rangle\frac{\partial}{\partial x}\langle n\rangle + \frac{\partial}{\partial x}\langle \tilde{v}_x\tilde{n}\rangle = D_0\frac{\partial^2}{\partial x^2}\langle n\rangle, \\ &\frac{\partial}{\partial t}\tilde{n} + \langle v_x\rangle\cdot\nabla\tilde{n} - D_0\frac{\partial^2}{\partial x^2}\tilde{n} + \tilde{v}_x\frac{\partial}{\partial x}\langle n\rangle = D_0\frac{\partial^2}{\partial y^2}\tilde{n}, \end{aligned} \qquad (3-9)$$

where we have dropped higher order terms.

We can define

$$\frac{d}{dt}\tilde{n} = \frac{\partial}{\partial t}\tilde{n} + \langle v_x\rangle\cdot\nabla\tilde{n} - D_0\frac{\partial^2}{\partial x^2}\tilde{n}. \qquad (3-10)$$

Since the width of the tube is much less than its length, $\partial_x \ll \partial_y$. So at a stationary state ($\partial_t = 0$), it is reasonable to neglect $d\tilde{n}/dt$. By balancing the remaining two terms of equation (3-9b), we obtain

$$\tilde{n}_{k_y} = -\frac{1}{k_y^2 D_0}\tilde{v}_{x_{k_y}}\frac{\partial}{\partial x}\langle n\rangle. \qquad (3-11)$$

Substituting equation (3-11) into equation (3-9a), we get

$$\frac{\partial}{\partial t}\langle n\rangle + \frac{\partial}{\partial x}\langle n\rangle + \frac{\partial}{\partial x}\sum_{k_y} -\frac{\left|\tilde{v}_{x_{k_y}}\right|^2}{k_y^2 D_0}\frac{\partial}{\partial x}\langle n\rangle = D_0\frac{\partial^2}{\partial x^2}\langle n\rangle. \qquad (3-12)$$

Clearly, according to equation (3-12), it is convenient to define

$$D_{eff,axial} = D_0 + D_{shear} = D_0 + \sum_{k_y} \frac{\left|\tilde{v}_{x_{k_y}}\right|^2}{k_y^2 D_0}. \qquad (3-13)$$

Since we are studying a laminar flow, the fluctuation level is of the same magnitude as the mean flow, i.e. $|\tilde{v}^2| \sim \langle v \rangle^2$. So $D_{shear} \sim v_0^2 L_\perp^2 / D_0 \sim P_e^2 D_0$. For a laminar flow, it is quite possible that $D_{shear} > D_0$ (actually, in this case, the Peclet number is about $\sqrt{48}$). Thus, the effective axial diffusivity is enhanced. *The fundamental character of the result that differential unidimensional convection and transverse diffusion yield a longitudinal diffusion process for downstream.* Taylor proposed that shear dispersion as a possible mechanism for distributing nutrients in blood flow. As I write this, I suddenly found a scary fact. Wait a minute, is D_{shear} irrelevant to shear rate?! *Though it can't be over-emphasized that shear is very important in this story, shear rate $\partial_y \bar{v}_x$ doesn't enter the final result!* After reading the supplement materials published on Canvas, I eventually found that since we take the spatial average over lateral direction, $\langle v_x \rangle$ has lost the information of shear, which has been buried in $\tilde{v}$ instead. Thus, $\tilde{v}$ is not the velocity fluctuation that we get used to. To restore the presence of shear, we should add an extra term $(\bar{v}_x(y) - \langle v_x \rangle)\partial_x \langle n \rangle$ to the L.H.S of equation (3-9b), balance it with $D_0 \partial_y^2 \tilde{n}$ and find the expression $\tilde{n}$. Note that this is a nontrivial modification because it vanishes when flow is uniform.

4. Percolation theory

Finally, after an interminable introduction (section 1 and section 2 explain why we are interested in $Ku > 1$ and percolation theory, respectively) and an exhausting detour (section 3 serves as a side story), here comes the entrée, i.e., percolation theory. As I said in section 2, in percolation, intrinsic and random properties of medium determine motion. *In other words, the medium is random while the motion of particles is deterministic.* A maze could be a rough example of

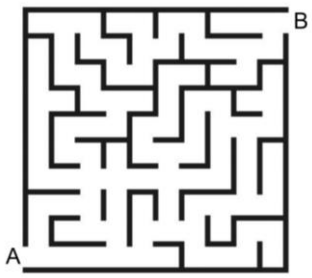

Figure 11 The structure of a maze looks stochastic. You can only go from A to B if these two points are really connected.

percolation. As shown in figure 11, particle or flow can traverse $A \rightarrow B$ only if there is an un-dammed, un-cut, self-avoiding (no circle in the trajectory, since it makes no contribution to the global transport) random walk connecting point A and B.

Another motivation for studying percolation is its relevance to fluid flow, which originates from Broadbent and Hammersley's research in 1950s [8]. Especially, we are interested in hydrology (like Hurst's work), transport/flow through porous media, and microscopic underpinnings of Darcy's law and Kozeny equation:

$$\boldsymbol{q} = -\frac{\kappa}{\mu}\nabla p, \qquad (4-1)$$

where $\boldsymbol{q}$ is flow flux, κ is permeability. Also, percolation cluster distribution is a measure of emergent order and its statistical characterization. Percolation is a simpler problem than avalanche distribution. Self-organized criticality is originally defined in terms of "percolation cluster" of single toppling (See BTW [9]). It is also a prototype of many-body, short range interaction system with universality, scaling, etc.

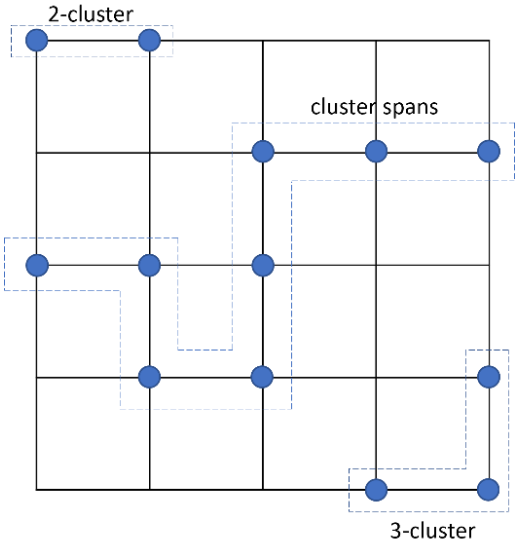

Figure 12 Clusters on a 2D square lattice.

Mathematically, it is easy to formulate percolation problem on a lattice. There are two ways to study percolation of a lattice: site percolation and bond percolation. For site percolation, every site of the lattice is either occupied with a probability p or unoccupied with a probability $(1-p)$. As illustrated in figure 12, on a 2D lattice, we can define a N-cluster by the number of occupied sites it includes. A cluster is bounded by a layer of unoccupied sites. For bond percolation, every site

of the lattice is occupied while each bond on the lattice is present with a probability p or absent with a probability $(1-p)$. It can be proved that a bond percolation L is equivalent to site percolation on the "covering lattice" L^*, but no vice-versa [10]. For example, in the case of a square lattice in figure 13, the covering lattice is formed by placing a site in L^* at the center of every bond in L and connecting these sites in L^* whose corresponding bonds share a common site in L. A closed bond in L is mapped into an occupied site in L^*.

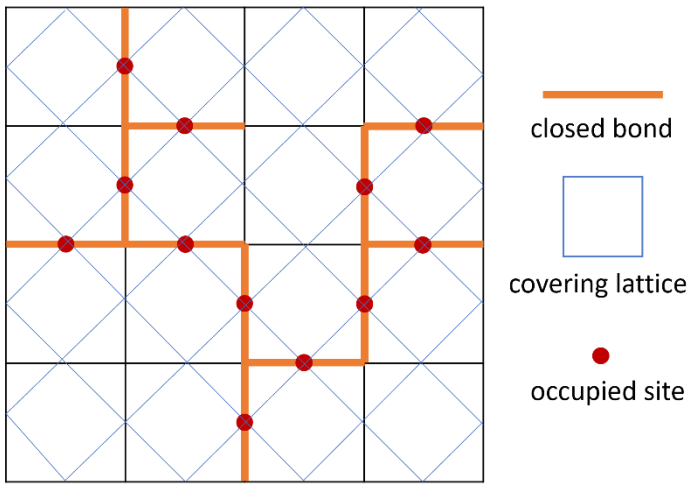

Figure 13 Mapping a bond percolation to a site percolation.

Consider a lattice of N sites ($N \gg 1$). The occupation probability is p, which is a tuning parameter of the system. When p is very small, only isolated small clusters appear. As p increases, larger and larger clusters form. Until p is greater than a critical value p_c, a large cluster spanning the whole lattice forms, corresponding to percolation. As we can see, this phenomenon owns the properties of phase transition, which is accompanied by critical exponents. *So what interests us is statistical characterization of these clusters as* $p \to p_c$. Another important question is, "How do I know it when I see it?" Specifically, how do we identify or visualize percolation in a simulation? Since percolation is intrinsically a static concept (i.e., a snapshot), we can analyze clustering, distribution in an image. The picture (figure 14) in Boffetta's work beautifully shows vorticity clustering in 2D turbulence, which appeals to intuition from percolation [11]. We can also introduce the concept of time to percolation. If we broadcast a sequence of cluster images, it should manifest avalanches, i.e., large clusters discharges across the system. In this note we mainly focus on site percolation. In the rest of this section, we will introduce the *scaling theory* of percolation.

Assume the probability of a site being occupied is p. A cluster containing s occupied sites is called

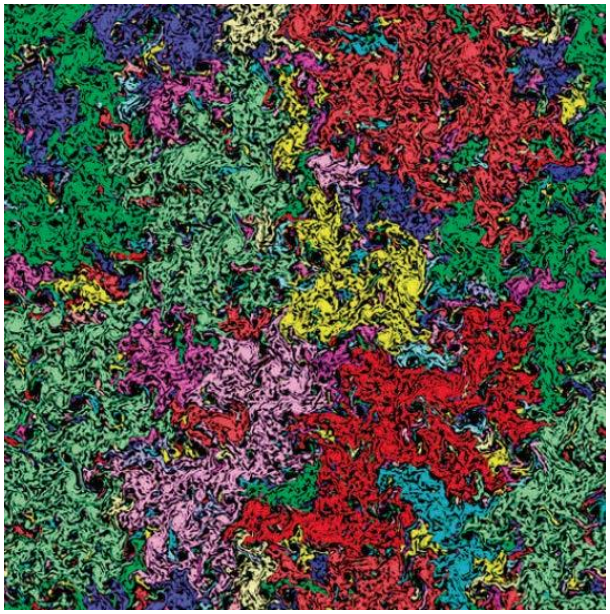

Figure 14 Illustration of vorticity clusters in Boffetta's simulation. These clusters are defined as connected regions with the same sign of vorticity. Different clusters are filled in different colors.

a s-cluster. To characterize the statistics of the lattice, we can define a new quantity n_s, which is the average number of s-clusters over the number of total sites. So $n_s(p)$ is a function of s and p. When $p < p_c$, $\sum_s n_s$ is the total number of clusters and $\sum_s s n_s$ is equal to p. *N.B., here s-clusters only refer to clusters containing a finite number of sites.* However, when $p > p_c$, clusters spanning the whole lattice emerges. Then we can define percolation probability p_∞, which is the fraction of occupied sites belonging to a percolation network. *It measures the "strength" of infinite network.* Therefore, for an arbitrary lattice site, it can be empty with a probability $(1-p)$, part of a percolation cluster with a probability pp_∞, or part of a finite cluster $p(1-p_\infty)$, which is equal to $\sum_s s n_s$. Then we have the relation

$$1 - p + pp_\infty + p(1 - p_\infty) = 1. \qquad (4-2)$$

Near p_c, one important observation is that the system has a divergent correlation length and a self-similar structure, i.e., which indicates a power law of $\sum_s n_s$, $\sum_s s n_s$, etc. Due to this fact, we can define several scaling exponents by following power laws

$$\begin{aligned}
&\sum_s n_s(p) \sim |p - p_0|^{2-\alpha}, \\
&\sum_s s n_s(p) \sim |p - p_c|^{\beta}, \\
&\sum_s s^2 n_s(p) \sim |p - p_c|^{-\gamma}, \\
&\epsilon(p) \sim |p - p_c|^{-\nu},
\end{aligned} \qquad (4-3)$$

where $\epsilon(p)$ is the correlation length. For 2D percolation, we have $\alpha \sim 0.7$, $\beta \sim 0.14$, $\gamma \sim 2.4$, and $\nu \sim 1.35$. *This phenomenon is also known as universality, because the values of these exponents are independent of the details of a specific site element. In addition, they are also irrelevant to the lattice structure, i.e., whether it is a square lattice or a triangular lattice doesn't matter.* However, we note that the first three power laws belong to n_s and its moments. In principle, we can define the moment of n_s all the way to infinite order. Does this mean we will get infinite number of scaling exponents? The answer is no. Quickly we can see all these scaling exponents can be derived from two scaling exponents.

For 1D percolation, the expression for n_s is

$$n_s = p^s (1-p)^2, \qquad (4-4)$$

which is easy to understand—p^s is the probability that s adjacent sites are occupied and $(1-p)^2$ is the probability that two ends are connected to two empty sites. Using equation (4-4), we can get

$$\sum_s n_s s = \sum_s p^s (1-p)^2 s = (1-p)^2 p \frac{d}{dp} \sum_s p^s = (1-p)^2 p \frac{d}{dp}\left(\frac{p}{1-p}\right) = p, \qquad (4-5)$$

which is not a surprise. Now define ω_s as the probability of s-cluster to which an arbitrary site belongs. Mathematically,

$$\omega_s = \frac{n_s s}{\sum_s n_s s}. \qquad (4-6)$$

So the average cluster size is

$$\bar{s} = \sum_s s \omega_s = \frac{\sum_s n_s s^2}{\sum_s n_s s}. \qquad (4-7)$$

Using the same trick we used for the calculation of $\sum_s sn_s$, we get

$$\bar{s} = \frac{\sum_s (1-p)^2 p^s s^2}{\sum_s (1-p)^2 p^s s} = \frac{1+p}{1-p}. \qquad (4-8)$$

Obviously, as $p \to p_c$, $\bar{s} \to \infty$, which means $p_c = 1$. If $p = 1 - \delta$, then $\bar{s}$ scales as $2/\delta$.

Things are more complex in the 2-dimensional case. For 1D percolation, $n_s \sim p^s$. So it is reasonable to assume that for 2D percolation we still have

$$n_s \sim e^{-cs}, \qquad (4-9)$$

where c is a function of $|p - p_c|$. But near criticality, 2D lattice also owns a self-similar structure, so n_s should also be proportional to $s^{-\tau}$. In a word, the scaling of n_s is

$$n_s \sim s^{-\tau} e^{-|p-p_c|^{1/\sigma} s}, \qquad (4-10)$$

which is a stretched exponential function. *The exponential part of the scaling defines effective cut-off on the range of cluster sizes, i.e., only clusters smaller than $|p - p_c|^{-1/\sigma}$ contribute to cluster average. The power law part of the scaling law reflects the self-similarity near criticality, i.e., $n_s \to s^{-\tau}$ as $p \to p_c$.* Equation (4-2) tells us that when $p \to p_c^+$,

$$pp_\infty + \sum_s sn_s = p. \qquad (4-11)$$

But at $p = p_c$, $p_\infty = 0$. So

$$\sum_s n_s(p_c) s = p_c. \qquad (4-12)$$

Plugging equation (4-12) into equation (4-11), we get

$$pp_\infty = \sum_s \big(n_s(p_c) - n_s(p)\big) s + O(p - p_c) \cong \sum_s s^{1-\tau} (1 - \exp(-cs)). \qquad (4-13)$$

Transforming the summation in equation (4-13) into an integral, we have

$$pp_\infty \sim c^{\tau-2} \int z^{2-\tau} e^{-z} dz = c^{\tau-2} \Gamma(3-\tau). \qquad (4-14)$$

Since $c \sim |p - p_c|^{1/\sigma}$, we can conclude

$$p_\infty \sim (p - p_c)^\beta = (p - p_c)^{\frac{(\tau-2)}{\sigma}}. \quad (4-15)$$

So $\beta = (\tau - 2)/\sigma$. The same strategy applies to the calculation of $\bar{s}$. According to equation (4-7), when $p \to p_c$, we have

$$\bar{s} = \frac{\sum_s s^2 n_s}{p_c} = \int ds n_s s^2 \sim c^{3-\tau} \int z^{2-\tau} e^{-z} dz \sim |p - p_c|^{-\gamma}, \quad (4-16)$$

where $\gamma = (3 - \tau)/\sigma$. Consider a more general case, the k-moment of s scales as

$$m_k = \sum_s s^k n_s \sim \int ds s^{k-\tau} e^{-cs} \sim c^{\tau-1-k} \int dz z^{k-\tau} e^{-z} \sim |p - p_c|^{(\tau-1-k)/\sigma}. \quad (4-17)$$

So σ and τ are the only two independent scaling exponents. If we know the σ and τ, we can obtain all the other scaling exponents.

Actually, to get these results, it is unnecessary to assume that $n_s \sim e^{-cs}$. Instead, we can assume

$$n_s \sim s^{-\tau} f[(p - p_c)s^\sigma], \quad (4-18)$$

where f is to be determined from computation. In this light, we have

$$\bar{s} \sim \int ds s^{2-\tau} f[(p - p_c)s^\sigma] \sim |p - p_c|^{-(3-\tau)/\sigma} \int dz z^{2-\tau} f(z) \sim |p - p_c|^{-(3-\tau)/\sigma}, \quad (4-19)$$

which is consistent with equation (4-16).

What? You ask how to get σ and τ? Well, you can get it by running a numerical simulation. But here I'd like to introduce a method called renormalization group (RG) theory that exploits the self-similarity of the system near the critical point [10]. Trust me, don't be scared by its big name. RG is not as hard as you expected.

A RG transformation always has two steps: (1) coarse graining or decimating; (2) rescaling parameters to map the coarse-grained system back to the original one. Suppose α is a parameter of the system, e.g., a scaling exponent defined in equation (4-33). After a mapping as described above, it becomes $\alpha^* = R(\alpha)$. Near a fixed point, system is self-similar, so

$$\alpha^* = R(\alpha) = \alpha, \quad (4-20)$$

which provides a way to calculate the value of α near criticality. Now let's take 2D triangular

lattice as an example. First, we break up the original lattice L into clusters of three sites each. As shown in figure 14, these clusters themselves form a new triangular lattice L' whose lattice constant is larger that of the original lattice by the factor $\sqrt{3}$. Then we coarse grain each cluster into a site in this new triangular lattice L' based on a "majority rule", which means this site in L' is occupied if the majority of the sites in the small cluster of L are occupied, and the cluster maps into an empty site otherwise. Then we rescale the lattice constant of L' to make it identical to the that of L.

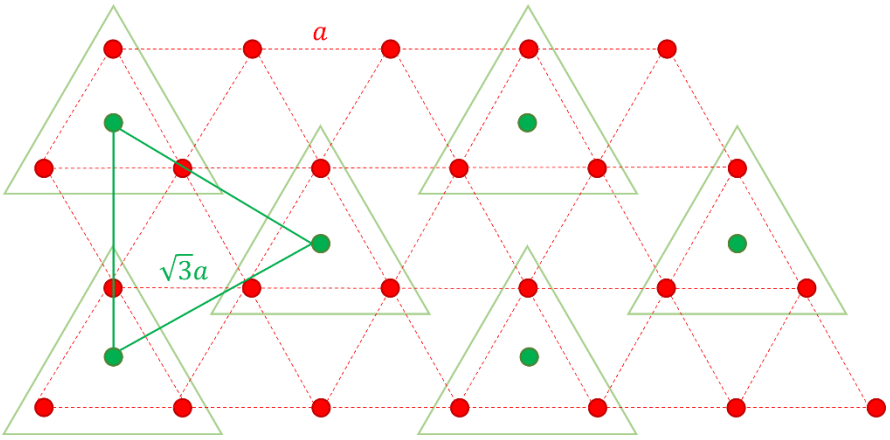

Figure 15 Illustration of the coarse graining of a triangular lattice

According to the majority rule, the probability that a site in L' is occupied is equal to the probability of at least two sites of the cluster in L are occupied. Then we have

$$p' = 3p^2(1-p) + p^3 = 3p^2 - 2p^3. \qquad (4-21)$$

Due to the self-similarity of the system near the critical point, $p' = p$. By solving equation (4-21), we get $p_c = 0.5$, which is exactly the accurate percolation threshold for 2D triangular lattice. As for scaling exponents, recall equation (4-3d)

$$\epsilon(p) \sim |p - p_c|^{-\nu}. \qquad (4-3d)$$

Let $p = p_c + \Delta$. After a RG transformation, we have

$$p'(p) \approx p_c + \left(\frac{\partial p'}{\partial p}\right)_{p=p_c} \Delta. \qquad (4-22)$$

Since we reduce the scale of L' by $\sqrt{3}$ in step (2), the correlation length is also reduced by $\sqrt{3}$. Plugging equation (4-22) into equation (4-3d), we obtain

$$\epsilon(p) = |p - p_c|^{-\nu} = \sqrt{3}\epsilon'(p') = \sqrt{3}\left(\frac{\partial p'}{\partial p}\right)_{p=p_c}^{-\nu} |p - p_c|^{-\nu}. \qquad (4-23)$$

Utilizing equation (4-21), we get

$$\nu = \frac{\ln\sqrt{3}}{\ln(\partial p'/\partial p)_{p=p_c}} = 1.3547\ldots, \qquad (4-24)$$

which is very close to the true value $\nu = 1.35$.

Now we go back to the percolation of magnetic field lines [5]. Different from the case we discussed in section 2 ($\langle A\rangle = 0, \langle A^2\rangle = A_0^2$), we now have a weak but non-zero mean field, i.e. $\langle B\rangle \neq 0$ and $\langle B\rangle \ll \tilde{B}$. *As shown in figure 16, the mean field is distorted by the small-scale fields. Mean field lines now look like sinews threading through a "soup" of cells.*

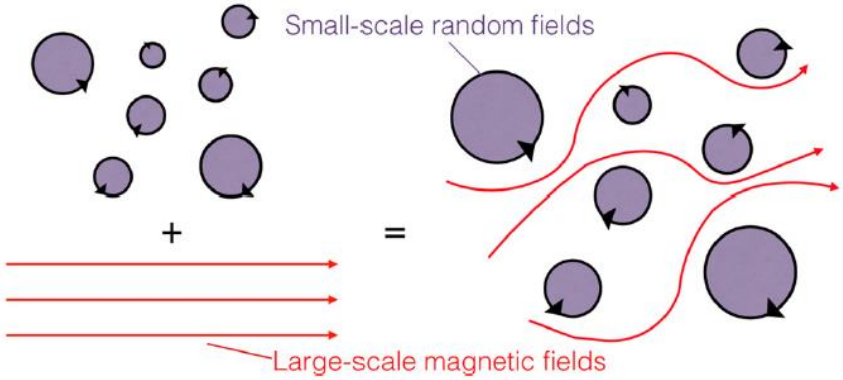

Figure 16 Percolation of mean field lines

The question is "does $\langle B\rangle$ percolate through the system as a, the size of the system, approaches infinity?" Since a is the largest spatial scale in this system, the minimum wave vector is $k_{min} = 2\pi/a$. Assume the spectrum of A is

$$\langle A^2\rangle_{\boldsymbol{k}} = \begin{cases} e^{-k^2/k_0^2}, k > k_0 \\ \left(\frac{k}{k_0}\right)^m, m > 0 \;\; k < k_0 \end{cases}. \qquad (4-25)$$

Then define the mean field as

$$\langle B\rangle = \left(\langle b^2\rangle_{k<1/a}\right)^{1/2}. \qquad (4-26)$$

Plugging equation (4-25) into equation (4-26), we get

$$\langle B\rangle = \left(\int_0^{1/a} dkkk^{2m}k^2\right)^{1/2} \cong (1/a)^{-m-2}. \qquad (4-27)$$

Clearly, when $m = -2$, $\langle B\rangle = const \neq 0$ as $a \to \infty$. Moreover, since $j_{z_{\boldsymbol{k}}} \cong k^2 A_{\boldsymbol{k}} \sim const$, we can conclude that *random current (i.e., white noise spectrum) will result in a percolating mean field.* More generally, we need $\langle j(\boldsymbol{x})j(\boldsymbol{x}+\boldsymbol{r})\rangle \geq 0$ (correlated currents) for percolating $\langle B\rangle$. It is easy to imagine that there is percolation for anti-correlated currents since fields they produce will cancel.

5. Conclusion

In this note, we explain why we are interested in $Ku > 1$ regime and why we should study percolation theory. We use resonance broadening theory to calculate the effective diffusivity of system under nonlinear scattering correction. But in the end, we prove that the system behaves more like percolation than diffusion. We also study systems intermediate between diffusion and percolation: Taylor cell problem and Taylor shear dispersion. Site percolation of lattice is studied by using scaling theory. Scaling exponents and critical occupation probability are calculated via renormalization group theory, which utilizes the self-similarity of the system near a relevant critical point. Finally, we study the percolation of mean magnetic field and conclude that a random current density will result in a percolating mean field.

References

[1]. Diamond, Patrick H., Sanae-I. Itoh, and Kimitaka Itoh. Modern Plasma Physics: Volume 1, Physical Kinetics of Turbulent Plasmas. Cambridge University Press, 2010.

[2]. Rechester, A. B., and M. N. Rosenbluth. "Electron heat transport in a tokamak with destroyed magnetic surfaces." In Hamiltonian Dynamical Systems, pp. 684-687. CRC Press, 2020.

[3]. Kadomtsev, B. B., and O. P. Pogutse. "Electron heat conductivity of the plasma across a'braided'magnetic field." Plasma Physics and Controlled Nuclear Fusion Research 1978, Volume 1 1 (1979): 649-662.

[4]. Taylor, J. B., and B. McNamara. "Plasma diffusion in two dimensions." The Physics of Fluids 14, no. 7 (1971): 1492-1499.

[5]. Zel'dovich, Y. B. "Percolation properties of a random two-dimensional stationary magnetic field." Pis'ma Zh. Eksp. Teor. Fiz. 38, No. 2, 51-54.

[6]. Rosenbluth, M. N., H. L. Berk, I. Doxas, and W. Horton. "Effective diffusion in laminar convective flows." The Physics of fluids 30, no. 9 (1987): 2636-2647.

[7]. Taylor, Geoffrey Ingram. "Dispersion of soluble matter in solvent flowing slowly through a tube." Proceedings of the Royal Society of London. Series A. Mathematical and Physical Sciences 219, no. 1137 (1953): 186-203.

[8]. Broadbent, Simon R., and John M. Hammersley. "Percolation processes: I. Crystals and mazes." In Mathematical proceedings of the Cambridge philosophical society, vol. 53, no. 3, pp. 629-641. Cambridge University Press, 1957.

[9]. Bak, Per, Chao Tang, and Kurt Wiesenfeld. "Self-organized criticality." Physical review A 38, no. 1 (1988): 364.

[10]. Creswick, Richard J., Horacio A. Farach, Charles P. Poole, and C. M. Poole. Introduction to renormalization group methods in physics. Wiley-Interscience, 1992.

[11]. Bernard, Denis, Guido Boffetta, Antonio Celani, and Gregory Falkovich. "Conformal invariance in two-dimensional turbulence." Nature Physics 2, no. 2 (2006): 124-128.